IET Science, Measurement & Technology

Research Article

IET Journals
The Institution of Engineering and Technology

Equivalent circuit for the thermal analysis of cables in non-vented vertical risers

ISSN 1751-8822
Received on 30th April 2014
Accepted on 7th November 2014
doi: 10.1049/iet-smt.2014.0127
www.ietdl.org

Imad Baker ✉, *Francisco de León*

Department of Electrical and Computer Engineering, Polytechnic School of Engineering, New York University, Brooklyn, NY 11201, USA
✉ *E-mail: ib563@nyu.edu*

Abstract: This study presents an alternative methodological approach for thermal rating of power cables installed in vertical risers covered by unvented circular protective guards. An analogue thermal-electrical circuit is proposed for the thermal analysis of cables inside vertical risers. The proposed equivalent analogue model is verified by means of indoor experiments and finite-element simulations with various cable and riser geometries for various load currents. Single cable and trefoil configurations are studied. Analysis performed on measured, simulated and calculated data establish the validity of the proposed model. Computations performed using the proposed method give results within 5% of measured conductor temperature. It is concluded that increasing riser height has minimal or insignificant impact on conductor temperature, whereas, reducing riser diameter, holding other variables constant increases conductor temperature and therefore reduces cable ampacity.

1 Introduction

Cable distribution systems frequently consist of underground sections and overhead sections that are connected through a short section (riser) secured on a pole and covered by a guard. The guard, in addition to preventing human accidents, provides protection to the high voltage cables from animals and the elements. This paper discusses the most commonly used riser construction for high voltage cables: unvented closed top and bottom. Commonly, the ampacity of the composite cable distribution system is limited by the thermal performance of this short section. The reason is that the heat transfer from the cable surface to the ambient is severely obstructed by the protective cable guard. Therefore the cable operating temperature increases and as a result its current carrying capacity reduces.

The IEC and the IEEE provide standardised methods and formulae for the thermal analysis of cables installed directly buried, inside duct banks, in filled or unfilled troughs, in air, in tunnels etc. The IEC standards lack of any method to directly solve the problem of cables in vertical protective risers. To rate cables in riser poles, the IEEE Std. 835 [1] relies on the work by Hartline and Black (1983) [2], which uses a correlation to calculate the average Nusselt number applicable for parallel flat plates and cylinders [3]. Both references [1, 2], neglect the important diameter-to-length ratio which sets the condition for the use of this correlation for cylinders ($D/L > 35/\mathrm{Gr}^{0.25}$). This condition is not met by the numerical example of the submarine cable presented in [2].

Moreover, the method of [2] stops short from providing a general model by failing to define a thermal resistance at locations within the thermal circuit where convection and radiation occur simultaneously. Anders (1996) updated the work of Hartline and Black by redefining the mathematical model [4]. Anders' model seems to be implemented in CYMCAP [5]. Our proposed model and method deliver better results than those of CYMCAP especially for trefoil configurations.

The experimental work done by Cress and Motlis [6] (1991) focused on collecting results from outdoor temperature-rise tests on submarine power cables protected by a vertical guard under specific solar radiation conditions. The data was used to compute the intensity of solar radiation and to verify a proprietary cable ampacity computer program. Authors did not present any formula or method for calculating ampacity for cables in vertical guards.

The original contributions of this paper are: (1) the development of an equivalent thermal-electrical analogue circuit for rating cables in riser poles in steady-state considering both convection and radiation simultaneously; (2) to propose an alternative simpler methodological approach (based on the developed model) for computing ampacity for power cables in vertical risers covered by protective guards by calculating conductor temperature for a given load current; (3) experimental verification of the proposed method, model and determine the effects of concentric against eccentric modelling of cables in riser poles.

For special and complex cable arrangements, such as: cables on riser poles, cables in open and covered trays, cables in tunnels and shafts and cables in shallow troughs [4], heat transfer mechanisms and heat transfer rates are greatly impacted by the installation geometries and conditions. The thermal performance of cables installed in riser poles is greatly dependent on the diameter of the guard, the intensity of the solar radiation, and the surface coefficient of solar absorption [7]. In this paper, various cable diameters, riser heights and riser diameters are investigated. Calculations performed employing the proposed circuit and method accurately predict the cable conductor, cable jacket, riser inner wall and riser outer wall temperature profile. Computed temperatures of cable conductor are within 5% of the measured temperatures for various riser heights, diameters and load currents which demonstrate the validity of the proposed circuit.

2 Equivalent thermal circuit

The solution of the heat transfer problem for cables installed in riser poles involves the following set of three non-linear equations [8]

The Navier–Stokes equation

$$\rho\frac{\partial u}{\partial t}+\rho(u\cdot\nabla)u=\nabla\cdot\left[-pR+\mu(\nabla u+(\nabla u)^{T})-\frac{2}{3}\mu(\nabla\cdot u)R\right]+\rho g \tag{1}$$

The continuity equation

$$\frac{\partial\rho}{\partial t}+\nabla\cdot(\rho u)=0 \tag{2}$$

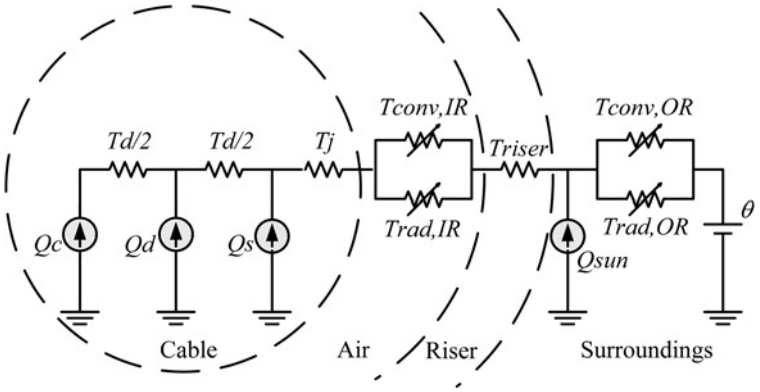

Fig. 1 *Equivalent thermal-electrical circuit for a power cable inside a riser indicating air thermal resistance to heat transfer by convection and radiation inside riser and outside riser*

The energy equation

$$\rho C_P \frac{\partial \theta^*}{\partial t} + \rho C_P \boldsymbol{u} \cdot \nabla \theta^* = \nabla \cdot (k \nabla \theta) + Q \tag{3}$$

where ρ is the density (kg/m^3), $\boldsymbol{u}$ is the air particle velocity vector (m/s), μ is dynamic viscosity (Pa.s), p is the pressure (Pa), g is gravitational acceleration (m/s^2), C_P is the specific heat capacity at constant pressure (J/(kg.K)), θ^* is the absolute temperature (K), Q is the heat dissipated (W/m), k is the thermal conductivity (W/m.k) and R is the radiation intensity.

Solving the three non-linear partial differential (1)–(3) simultaneously can be done numerically with finite elements (FEM). However, FEM simulations are very time consuming when natural convection is involved [8]. The alternative proposed in this paper is to use an equivalent thermal-electrical analogue circuit. The circuit accounts for the conduction of heat from the internal sources within the cable and riser system to the outer surface of the cable and to the outer surface of the riser through the layers of the cable and the riser. It also accounts for the convective and radiative heat transfer from the outer surface of the cable to the inner wall of the riser and from the outer surface of the riser to the surroundings.

Fig. 1 shows the proposed circuit representing a power cable housed inside a riser. Q_c, Q_d and Q_s are: Joule losses because of load current in the conductor, dielectric losses in insulation and sheath losses in metallic sheath, respectively. The resistances of the circuit are computed in the following section from first thermodynamics principles.

Analogous to current flow in electric circuits governed by Ohm's law, the transfer of heat Q through the cable, riser and surroundings is governed by

$$Q = \frac{\Delta \theta}{T} \tag{4}$$

where T is the thermal resistance of the layer in °C.m/W and $\Delta\theta$ is the temperature drop across the layer that drives the heat flow given in °C.

3 Heat transfer in vertical slender cylinders

Heat generated inside the cable travels from the conductor and other heat sources to the surroundings by conduction, convection and radiation. Heat flow is opposed by the thermal resistance T of the non-metallic layers. Metallic layers have much higher thermal conductivity and therefore their resistance is negligible in steady state.

3.1 Conduction

In cables and risers, conductive thermal resistance is present in all non-metallic layers: cable insulation, jacket and non-metal riser. Calculations of thermal resistance to heat flow by conduction because of cable insulation T_d, outer jacket layer T_j and non-metal riser T_{riser} are given by [9]

$$T = \frac{\ln (r_o/r_i)}{2\pi k} \tag{5}$$

where, r_o and r_i are the outer and the inner radii of the layer, respectively, as in (3) k is the thermal conductivity.

3.2 Dual convection and radiation

Heat transfers from the cable jacket to the inner wall of the riser through air by means of convection and radiation. Similarly, heat transfers from the outer surface of the riser to the surroundings by convection and radiation. At both locations, convection and radiation occur simultaneously and their total effect is additive. Therefore in the thermal-electrical analogy, air thermal resistance for both radiation and convection is presented in parallel to account for convection and radiation heat transfers simultaneously as presented in Fig. 1. Air thermal resistance to heat flow by convection from cable surface to riser inner wall $T_{\text{Conv,IR}}$ is given by

$$T_{\text{Conv,IR}} = \frac{1}{A_s h_s} \tag{6}$$

where h_s is the convective heat transfer coefficient of the cable surface and is defined as

$$h_s = \frac{\overline{\text{Nu}}}{L} k_{\text{air}} \tag{7}$$

k_{air} is the thermal conductivity of air (W/m.K) and is provided in the literature (see e.g. [8]) and must be calculated at proper temperature

$$\theta_{f1} = (\theta_s + \theta_{\text{IR}} + \theta)/3) \tag{8}$$

θ_s is the cable surface temperature, θ_{IR} is the riser inner wall temperature and θ is the ambient temperature.

A comprehensive literature research was performed on the calculation of the average Nusselt number $\overline{\text{Nu}}$ for natural convection from vertical slender cylinders that best fits our model; see for example [10–14] and [17–20]. Free convective heat transfer from vertical slender cylinders and flat vertical plates has been studied intensively as the understanding of this phenomenon is critical in the design of many engineering pieces of equipment. The results of convective heat transfer for vertical cylinder were first obtained by Sparrow and Gregg [13] in 1956 for Pr = 1 and Pr = 0.72. These results were extended by Cebeci in 1974 [12] for Pr = 0.01 to 100. Cebeci presented his experimental results on the effect of the cylinder curvature parameter on the cylinder to flat

plate in tabular format. Numerical data of Cebeci for Pr = 0.72 (air) can be approximated with the following correlation [11]

$$\overline{\mathrm{Nu}} = \overline{N}_{u-\mathrm{FP}}*\left(1 + 0.300\left[32^{0.5}(G_H)^{-0.25}\left(\frac{L}{D}\right)\right]\right)^{0.909} \quad (9)$$

where D is the surface outer diameter, $\overline{\mathrm{Nu}}$ is the average laminar Nusselt number for a vertical cylinder and $\overline{N}_{u-\mathrm{FP}}$ is the average laminar Nusselt number for a flat plate which is given by the known correlations of Churchill and Chu [14], and valid for Rayleigh numbers $0.1 < Ra_H < 10^{12}$ and for almost all Prandtl numbers

$$\overline{N}_{u-\mathrm{FP}} = \left[0.825 + \frac{0.387Ra_H^{1/6}}{[1 + (0.492/P_r)^{9/16}]^{8/27}}\right]^2 \quad (10)$$

where G_H and Ra_H are Garshoff and Reynolds dimensionless numbers, respectively, and defined in Appendix 2.

The radiative heat transfer from the cable surface to the inner wall of the riser $q_{\mathrm{rad},s-\mathrm{IR}}$ in terms of the shape factor is given by [17]

$$q_{\mathrm{rad},s-\mathrm{IR}} = \sigma\varepsilon A_s\left(\theta_s^{*4} - \theta_{\mathrm{IR}}^{*4}\right) \quad (11)$$

where σ is the Stefan–Boltzmann constant, ε is the radiation emissivity of the surface with area A_s, θ_s^* and θ_{IR}^* are the absolute temperatures of the cable surface and the inner radius of the riser, respectively.

Air thermal resistance to heat transfer by radiation from the surface of the cable to the inner surface of the riser $T_{\mathrm{Rad,IR}}$ is calculated using

$$T_{\mathrm{Rad,IR}} = \frac{1}{h_{\mathrm{rad}\ S-\mathrm{IR}}A_s} \quad (12)$$

where $h_{\mathrm{rad}\ S-\mathrm{IR}}$ the radiative heat-transfer coefficient and is given by [16, 17] by re-writing (11) as follows

$$q_{\mathrm{rad},s-\mathrm{IR}} = h_{\mathrm{rad}\ S-\mathrm{IR}}A_s\left(\theta_s^* - \theta_{\mathrm{IR}}^*\right) \quad (13)$$

Therefore

$$h_{\mathrm{rad}\ S-\mathrm{IR}} = \varepsilon\sigma\left(\theta_s^* + \theta_{\mathrm{IR}}^*\right)\left(\theta_s^{*2} + \theta_{\mathrm{IR}}^{*2}\right) \quad (14a)$$

ε is replaced by the radiation shape factor which is also referred to as the effective emissivity of the cable/riser system and value is given as [1]

$$F_{s,\mathrm{IR}} = \varepsilon_{\mathrm{eff}} = \frac{1}{((1/\varepsilon_s) + (D_s/D_{\mathrm{IR}})((1/\varepsilon_{\mathrm{IR}}) - 1))} \quad (14b)$$

where ε_s is cable surface emissivity, $\varepsilon_{\mathrm{IR}}$ is riser inner wall emissivity, D_s is cable diameter and D_{IR} is riser inner diameter.

Similarly, heat transfer from the outer surface of the riser to the surroundings takes place by convection and radiation, which occur simultaneously and presented in parallel in Fig. 1. Mathematically, air thermal resistance to heat transfer by convection outside riser (OR) is computed following the same steps used to calculate air thermal resistance to heat transfer by convection inside riser (IR) and is given by

$$T_{\mathrm{Conv,OR}} = \frac{1}{A_R h_R} \quad (15)$$

where, the convective heat-transfer coefficient h_R from outer surface of the riser with area A_R is found by utilising (7)–(10). Air properties are calculated with the correct film temperature given by

$$\theta_{f2} = ((\theta_{\mathrm{OR}} + \theta))/2) \quad (16)$$

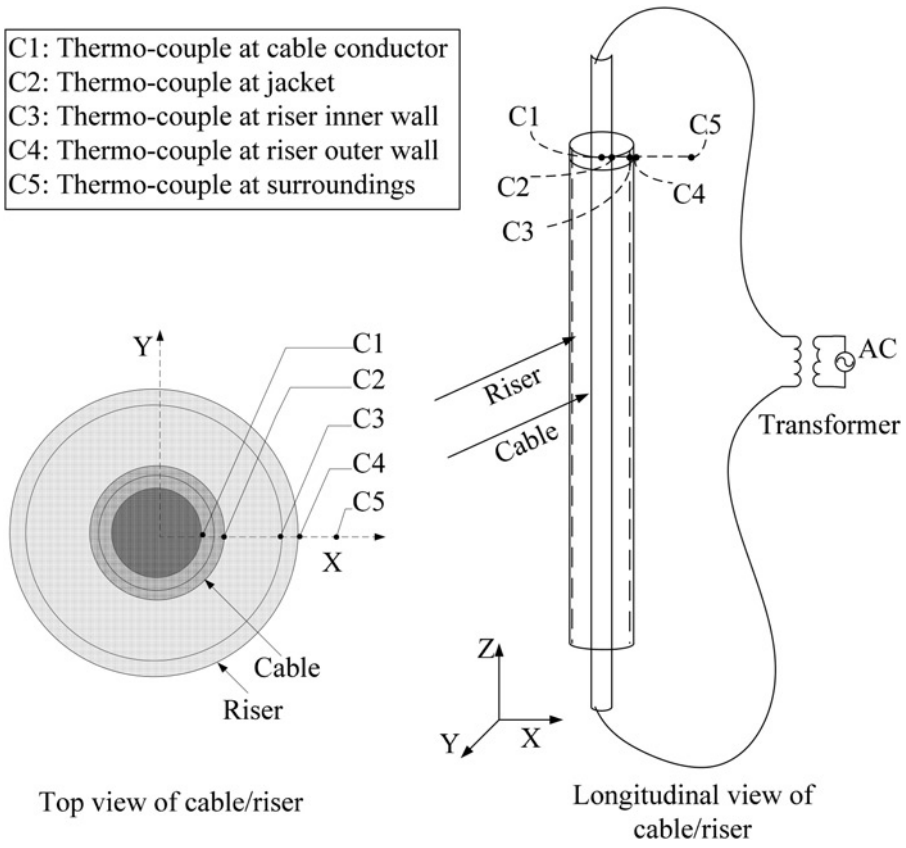

Fig. 2 *Indoor experiment setup showing longitudinal and top views of a cable inside a closed (top and bottom) vertical riser*

IET Sci. Meas. Technol., 2015, Vol. 9, Iss. 5, pp. 606–614

Air thermal resistance to heat transfer by radiation from outer radius of the riser to surroundings is calculated by

$$T_{\text{Rad,OR}} = \frac{1}{A_R h_{\text{rad OR}-\text{Surr}}} \tag{17}$$

Assuming that the riser is a small body enclosed by the surroundings, the radiative heat-transfer coefficient $h_{\text{rad OR}-\text{Surr}}$ from outer surface of the riser to surroundings is found in a similar fashion as $h_{\text{rad }S-\text{IR}}$ by utilising (13) and (14a). Where ε is the surface emissivity of the riser material, A_R is the riser outer surface area and θ_{OR} is the temperature of the riser outer surface.

4 Experiments

To establish the validity of the proposed model, several indoor experiments were performed while varying riser height, inner/outer diameter and load current. Single cable construction and trefoil formations were used for experimentation. Load current was provided by means of the secondary windings of a 25 kVA transformer shorted by the cable. For a single cable inside the riser, five thermo-couples were installed at different locations at the top of the cable/riser setup as shown in Fig. 2. Temperatures of the conductor, jacket, riser inner wall, riser outer wall and ambient were collected over several hours. Enough time was given to allow the system to set into steady-state for at least four hours. Thermo-couple C5 recording surroundings temperature (ambient) was placed around 50 centimetres away from the riser. Both ends of the riser were closed with rubber caps and the cable ran through a very tight opening through the centre of the caps to prevent heat from escaping and to ensure cable and riser are concentric. For experiments with three trefoil cables, the conductor and jacket temperatures were recorded for each cable.

5 Results and analysis

Two cable types (A and B) and two riser types (I and II) were used in the experiments and simulations. Their dimensions and construction materials are given in Appendix 1. The first set of experiments used a 1 m long PVC riser type I and a single cable of type A. Seven independent experiments varying the current from 200 to 500 A were performed with resolution of 50 A. For each current, a separate experiment was performed starting from 0 A and ramped up to targeted load current. Temperature-loggers sampled every second and recoded data 20 min prior to applying current, recorded the transient and went up to 4 hours after thermal steady-state is reached. On average single cable experiments run for 8 h. Fig. 3*a* shows the recorded cable and riser temperature profile in °C as a function of time with 500 A applied.

Measured steady-state conductor temperatures for various load currents are plotted as a function of applied load current as shown in Fig. 3*b*. Measured and calculated conductor temperatures are in agreement with maximum difference of 4% which clearly proves the validity of the proposed model.

Fig. 3*c* shows the temperature profile of the cable and riser system for the 450 A experiment. Analysis of the measured and calculated data shows a match of the cable and riser temperature profile proving the validity of the proposed circuit. IR and OR represent the inner radius (wall) and the outer radius of the riser, respectively.

More experiments were conducted using a single cable of type A inside a 2 m long type I riser. As before the current was varied from 200 to 500 A. Measured and calculated results have differences of less than 4%. The results are not shown, but they are almost identical to those of Fig. 3*b*. In fact, from the analysis of the results obtained from the experiments with 1 and 2 m risers, it is found that varying riser height has insignificant effect on conductor temperature. Fig. 4 shows conductor temperature change ($\Delta\theta$) as a function of load current for 1 and 2 m risers.

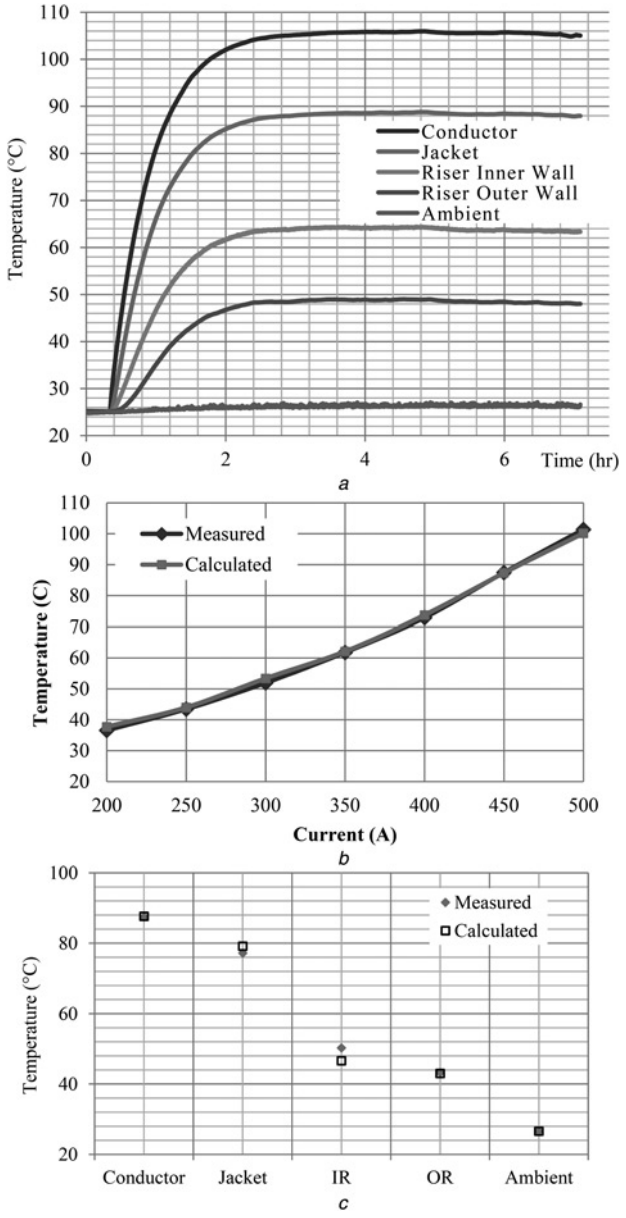

Fig. 3 *Temparture profile, measured and calculated conductor temperatures*

a Temperature profile as a function of time for 1 m long riser type-I and cable type-A with 500 A applied
b Measured and calculated conductor temperatures using 1 m long riser type-I and cable type-A for various load currents
c Measured and calculated temperature profiles for 1 m long riser type I and cable type A with 450 A applied

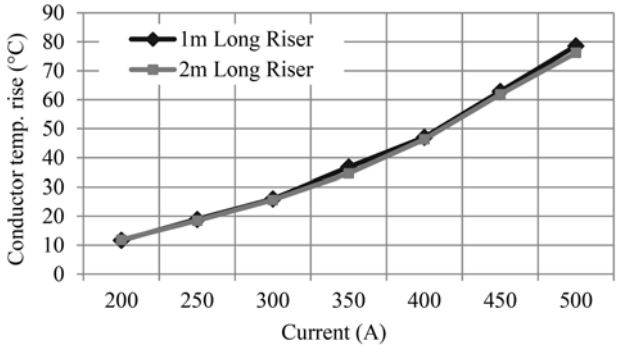

Fig. 4 *Measured temperature rise ($\Delta\theta$) of cable conductor as a function of load current for 1 and 2 m risers*

Table 1 Measured, CYMCAP and model temperature for a wide riser (Type II) and a single cable (Type A)

Current, A	Measured temp., °C	CYMCAP		Proposed model (Fig. 1)		Ambient, °C
		Temp., °C	% Error	Temp., °C	% Error	
200	36.8	36.2	1.6	37.4	1.6	26.0
250	42.7	41.8	2.1	42.5	0.4	26.1
300	49.5	48.1	2.8	49.2	0.6	26.0
350	57.8	56.0	3.1	57.3	0.7	26.2
400	67.9	65.0	4.2	66.8	1.6	26.4
450	80.2	75.3	6.10	77.6	3.2	26.6
500	95.0	87.1	8.3	90.2	5.0	27.0

Another set of experiments was performed using a 1 m long riser of wider diameter (type II) with a single cable type A and again varying the current from 200 to 500 A. The results of the core temperature from experiments, calculated with CYMCAP and calculated with our model are compared in Table 1. The proposed method shows smaller errors with respect to measured data (max. 5.0%), whereas CYMCAP provides a larger error of up to 8.3%. The differences between the measured values and CYMCAP results are possibly because of the surface emissivity for the PVC riser. CYMCAP uses emissivity of 0.9 which is hard-coded and cannot be changed by the user, wheras the standard value for PVC is 0.6 [19].

Increasing riser diameter leads to a reduced conductor temperature as shown in Fig. 5, which presents conductor temperature rise ($\Delta\theta$) for two different riser diameters as a function of applied current. Analysing the results, it is found that conductor temperature is mainly reduced because of the reduced air thermal resistance to convection and radiation between riser outer surface and surroundings as shown in Table 2. Both thermal resistances are inverse functions of the external area; see (15) and (17).

Further analysis of the results reveals that increasing riser diameter leads to increasing the percent heat transfer by radiation and reducing the percent heat transfer by convection (see Table 2).

6 Numerical example

6.1 Calculation procedure

The purpose of the numerical example is to illustrate the required steps one has to follow to calculate the temperature profile for a given cable and riser system utilising the proposed method. A flow diagram is provided in Fig. 6 illustrating these steps. To clearly illustrate the process, we will consider a 2 m long electric power cable type-A with copper conductor, EPR insulation and ethylene-propylene rubber serving (jacket), enclosed in a shaded circular non-vented PVC riser (see Fig. 8). Ambient temperature is $\theta = 25.16$°C. For cables with metallic sheaths and armours, the process remains the same but requires finding heat generated by these additional metallic layers and formulae are provided in IEC 60287-1-1.

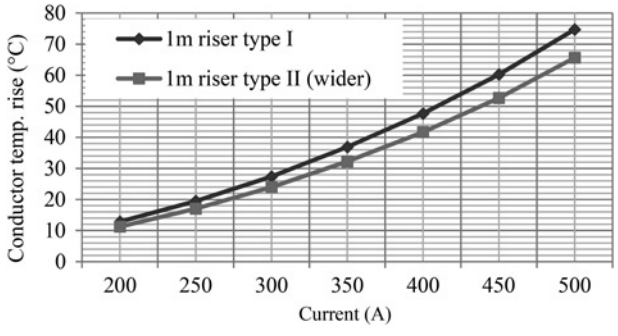

Fig. 5 *Measured temperature rise ($\Delta\theta$) of cable conductor for two different riser diameters as a function of load current*

The physical and thermal properties for the cable and riser are listed in Appendix 2.

Table 2 Calculated air thermal resistance to convection and radiation inside and OR for 500 A load current

Location	2 m type I riser	1 m type I riser	1 m type II riser
Tconv, s_IR [°C m/Q]	2.28	2.31	2.30
Trad, s_IR [°C m/Q]	2.65	2.65	2.83
Tconv, OR_amb [°C m/W]	1.22	1.20	0.78
Trad, OR_amb [°C m/W]	1.31	1.32	0.71
convection	51.8%	52.2%	47.6%
radiation	48.2%	47.8%	52.4%

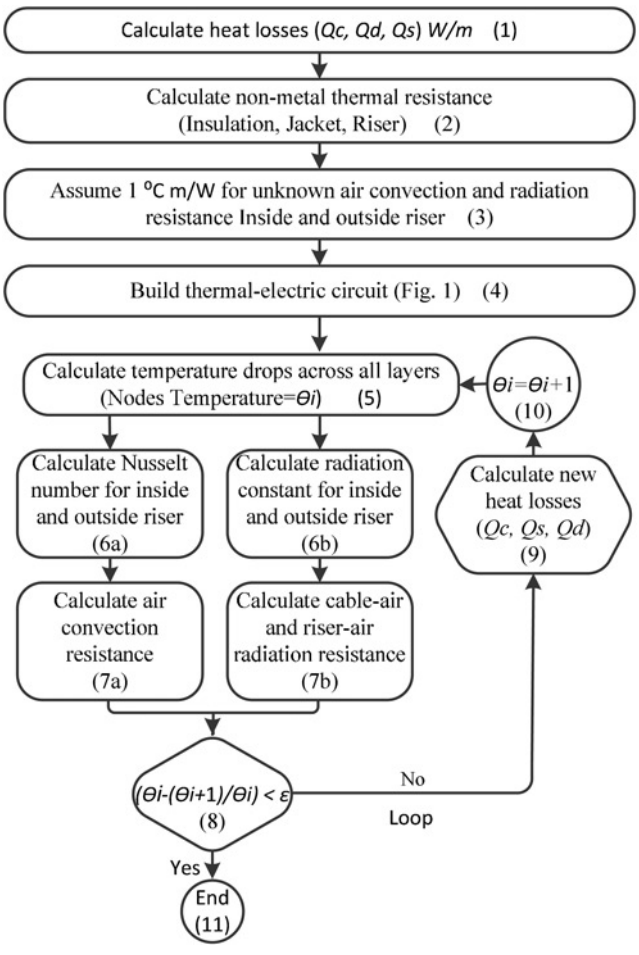

Fig. 6 *Flow diagram demonstrates the steps required for calculating the temperature profile for a given cable and riser system*

IET Sci. Meas. Technol., 2015, Vol. 9, Iss. 5, pp. 606–614

The calculation of Q_c, because of Joule losses in copper conductor requires knowledge of the conductor temperature to compute the electrical resistance. To start, one can assume a sensible temperature. Every time the convergence criterion is not met, we use the new calculated temperature and re-calculate the conductor *ac* resistance and then adjust Q_c accordingly and repeat steps until convergence. The steps shown in the block diagram of Fig. 6 are explained next:

Block 1: Assuming a starting temperature of 90°C, conductor resistance $R_{c,\mathrm{ac}} = 1.2552 \times 10^{-4}\,\Omega$/m, therefore heat loss $Q_c = 500^2 \times 1.2552 \times 10^{-4} = 31.38$ W/m, and $Q_{\mathrm{sun}} = 0$ (shaded riser).

Block 2: From (5), we calculate insulation, jacket and riser thermal resistances

$$T_{d/2} = \frac{\ln(9.6/7.6)}{2\pi 0.20} = 0.0932^{\circ}\mathrm{C\ m/W}$$

$$T_j = \frac{\ln(11.6/9.6)}{2\pi 0.20} = 0.1509^{\circ}\mathrm{C\ m/W}$$

$$T_{\mathrm{riser}} = \frac{\ln(30.10/25.59)}{2\pi 0.1667} = 0.1561^{\circ}\mathrm{C\ m/W}$$

Block 3: We assume $T_{\mathrm{conv\ IR}}$, $T_{\mathrm{Rad\ IR}}$, $T_{\mathrm{conv\ OR}}$ and $T_{\mathrm{Rad\ OR}} =$ 1°C m/W each.

Block 4: Build circuit as in Fig. 1.

Block 5: Using electric circuit analysis, we calculate node temperatures ($\theta_c = 74.16$°C, $\theta_s = 63.08$°C, $\theta_{\mathrm{IR}} = 46.66$°C and $\theta_{\mathrm{OR}} =$ 41.54°C).

Blocks 6a and 7a: Utilising the new conductor temperature ($\theta_c =$ 74.16°C), calculate air thermal resistance to convection inside and outside riser:

(a) From (21) and (22) find Garshoff and Reynolds numbers

$$G_H = 1.35 \times 10^{10} \text{ and } Ra_H = 9.62 \times 10^{9}$$

(b) Using (10), evaluate $\overline{N}_{u-\mathrm{FP}} = 249.2$

(c) Therefore (9) yields average Nusselt number for cylinder $\overline{\mathrm{Nu}} = 352.9$

(d) Substituting in (7) gives the convective heat transfer coefficient $h_s = 4.81$ W/°C m^2

(e) Using (6) find air thermal resistance between cable jacket and riser inner wall, $T_{\mathrm{Conv,\ IR}} = 2.85$°C m/W

(f) Repeat a) through e) to find air thermal resistance OR, $T_{\mathrm{Conv,OR}} =$ 1.31°C m/W

Block 6b and 7b: Utilising new conductor temperature ($\theta_c = 74.16$° C) compute air thermal resistance to radiation inside and OR using (11)–(14b) and (17): $T_{\mathrm{Rad,IR}} = 2.82$°C m/W and $T_{\mathrm{Rad,OR}} = 1.34$°C m/W.

Block 8: Check convergence criterion: $\theta_c < \in$, where $\Delta\theta_c = |(\text{old temp} - \text{new temp})|$ and $\in$ is tolerance representing acceptable temperature change (e.g. $\in = 0.050$°C). $\Delta\theta_c = |(90^{\circ}\mathrm{C} - 74.16^{\circ}\mathrm{C})| =$ 15.84°C.

Table 3 Numerical example results of all iterations taken to calculate final temperatures and air thermal resistances

Iteration	1	2	3	4
$R_{c,\mathrm{ac}}$ Ω/m	1.31×10^{-4}	1.25×10^{-4}	1.36×10^{-4}	1.35×10^{-4}
Q_c W/m	32.84	31.26	34.06	33.88
$T_{\mathrm{Conv,IR}}$ °C m/W	1	2.85	2.26	2.32
$T_{\mathrm{Rad,IR}}$ °C m/W	1	2.41	2.08	2.09
$T_{\mathrm{Conv,OR}}$ °C m/W	1	1.31	1.22	1.21
$T_{\mathrm{Rad,OR}}$ °C m/W	1	1.34	1.31	1.31
θ_c °C	74.16	102.23	100.49	100.54
θ_s °C	63.08	91.68	89.00	89.11
θ_{IR} °C	46.66	50.76	52.07	51.76
θ_{OR} °C	41.54	45.88	46.75	46.47
$\theta_c < \varepsilon = 0.05$°C	No	No	No	Yes

Table 4 Measured and calculated results of 2 m long cable carrying 500 A load current

	Measured	Calculated	Difference, %
conductor	101.35	100.54	0.79
jacket	88.99	89.11	0.13
riser inner wall	53.60	51.77	3.42
riser outer wall	44.28	46.47	4.78
ambient	25.16	25.16	–

Loop: Since $\Delta\theta_c = 15.84^{\circ}\mathrm{C} > \in$, using new calculated conductor temperature $\theta_c = 74.16$°C, re-calculate conductor *ac* resistance and $Q_c = 31.26$ W/m. Insert calculated air thermal resistances and new heat loss into circuit of Fig. 1 and repeat process until convergence criterion is met.

For this specific example, procedure converged after four iterations yielding a conductor temperature $\theta_c = 100.54$°C for a load current of 500 A as shown in Table 3.

Results of the numerical example match the measured data obtained from indoor experiment using cable type-A and 500 A applied. Table 4 shows measured and calculated temperature profile for the cable/riser used in the example.

6.2 Comparison with directly buried and cables in air

Cable type B is used for a comparative study on the effect of closed risers on cable ampacity against cables directly buried in native soil and against cables installed in free air. Using our model and method, it is calculated that cable B installed inside a shaded riser of 4 inch inner diameter and ambient temperature 25°C, can carry a maximum current of 1230 A, whereas the same cable under same ambient temperature, can carry up to 1,475 A if directly burred in native soil at a typical 1 m depth and rho = 0.9 and a maximum current of 1,640 A if installed shaded in free air, showing a severe reduction in cable ampacity because of the use of non-vented risers. Therefore as it is commonly the case, the short riser section is the bottleneck of the cable transmission network.

7 FEM simulations

A large number of lab experiments were performed using cable type A and risers types I and II. To gauge the scopes and limitations of the proposed model, hundreds of three-dimensional (3D) FEM simulations using COMSOL multi-physics 4.3 were performed. COMSOL supports all fundamental mechanisms of heat transfer necessary for the representation of power cables inside vertical risers [8]. The conjugate heat-transfer module with time-dependent segregated solvers was used. Anywhere between 196 000 and 1 968 000 triangular mesh elements and 27 000 to 259 000 boundary elements were used, depending on the length and the complexity of the cable/riser structure. Starting at an ambient temperature of 20°C, load current is applied to the cable conductor through a step function. Simulations ran from 3 to 8 h to compute

Table 5 COMSOL against CYMCAP and model using cable B and riser II

Current, A	COMSOL temp, °C	CYMCAP		Proposed circuit (Fig. 1)	
		Temp., °C	% Error	Temp., °C	% Error
700	43.06	40.60	5.71	41.81	2.88
800	49.23	46.70	5.14	48.06	2.36
900	56.08	53.50	4.60	55.12	1.70
1000	63.70	61.10	4.08	62.89	1.26
1100	72.20	69.50	3.73	71.55	0.89
1200	81.53	78.70	3.47	81.07	0.55
1300	91.85	88.80	3.32	91.52	0.35

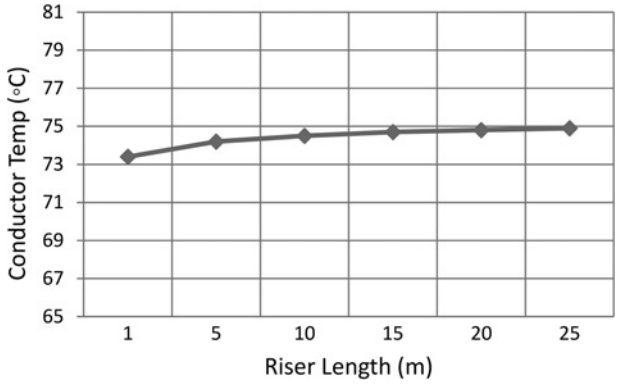

Fig. 7 *Simulated results for Cable A carrying a constant load current (400 A) inside riser-I while increasing riser length 1 to 25 m at ambient 26.4°C*

1–3 days of actual time using a server that has 24 cores in its central processing unit clocking at 3.33 GHz and with 192 GB of DDR3 RAM. A sample simulation case using cable type B and riser type II is shown in Table 5.

Additional parametric simulations were performed on cable B with different materials: unfilled XLPE insulation, aluminium sheath, and PVC jacket installed inside PVC risers of different diameters (American standard ducts 3, 4 and 5 inch nominal diameter were simulated), ambient temperature of 25°C and varying load current from 600 to 1200 A. Results are not shown, but using our proposed model and method, the computed conductor temperatures are within 0–2.8°C from simulated results, proving the validity of the proposed circuit.

Once the 3D FEM simulations have been validated experimentally for risers of 1 and 2 m, FEM simulations are used to produce results for risers with lengths of 5, 10 and 25 m. Simulated results for cable A inside riser type I is shown in Fig. 7. The conclusion is that the length of the riser insignificant impact (under 2%) on the temperature of the conductor.

Further analysis done on the computed data obtained above from cable B, found that for the same load current (1200 A), increasing the riser outer diameter has an inverse effect on the surface of the riser natural convection heat transfer coefficient h_R and therefore reducing air thermal resistance with increased riser diameter, and as a result, lower conductor temperature; see Fig. 8.

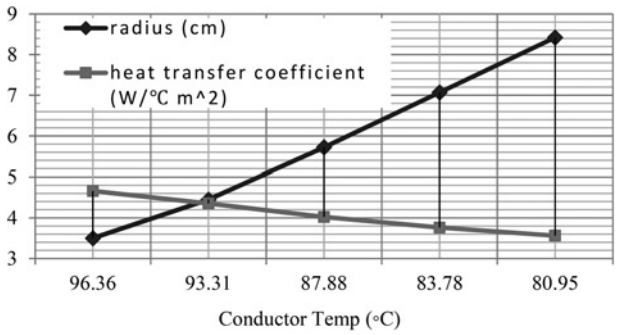

Fig. 8 *Cable B carrying a constant load current (1200 A) inside risers of different widths, increasing riser outer radius leads to a reduced heat transfer coefficient and in effect reduces conductor temperature*

Table 6 Measured temperature change of concentric and eccentric cable/riser of 1 m cable A riser I

Current, A	Conductor temp., rise, Concentric	Conductor temp., rise, Eccentric	Degrees difference, °C
200	11.65	12.08	−0.42
250	18.90	18.48	0.41
300	25.94	26.36	−0.42
350	36.76	36.76	0.00
400	47.03	47.97	−0.93
450	60.83	61.1	−0.27

8 Concentric against Eccentric modelling

The need to investigate concentric against eccentric cable and riser configuration arises from the fact that in practical applications it is very difficult to maintain cables inside riser in a concentric configuration. Therefore it is important to understand the impact that cables touching inner wall of riser will have on the conductor temperature. We have assumed concentric configuration in the numerical examples for calculations purposes and here investigate experimentally the effect that eccentric cables/riser have on conductor temperature. Measured temperature change using concentric and eccentric cable type-A and riser type-I are shown in Table 6.

Analysing the results provided in Table 6, conductor temperature at most changed by (–0.93°C) for cables/riser that are eccentric (touching) which is also within acceptable range of the measuring equipment errors. However, jacket and riser temperatures may suffer higher temperature changes and inhomogeneous temperature distributions depending on the point of contact between cable jacket and riser inner wall. Therefore it is safe to conclude that conductor temperature is not impacted significantly when cables touch the inside wall of the riser.

9 Trefoil configuration

Three cables of type A in trefoil configuration and riser type II were used in experiments. The proposed model of Fig. 1 applies to a single cable inside a closed riser. However, for the three cables can be replaced with a thermally equivalent single cable of a radius [1] as

$$r_{3\ \text{cables equivalent}} = 2.15 r_{1\ \text{cable}} \tag{18}$$

Thermal resistance of each of the equivalent cable layers given by [2]

$$T_{3\ \text{cables equivalent}} = (7/18) T_{1\ \text{cable}} \tag{19}$$

and total heat loss is

$$Q_{\text{total loss of 3 cables}} = 3 Q_{\text{total loss of a single cable}} \tag{20}$$

Obtained results from measurements, calculated and CYMCAP for

Table 7 Measured, calculated and CYMCAP conductor temperature for 3 cables in trefoil

Current, A	Measured temp., °C	CYMCAP		Proposed circuit (Fig. 1)		Ambient, °C
		Temp., °C	% Error	Temp., °C	% Error	
250	55.2	53.7	2.7	56.0	1.4	26.7
300	67.0	64.6	3.5	67.8	1.1	26.3
350	83.0	77.8	6.2	82.1	1.0	26.3
400	103.1	94.6	8.2	100.2	2.8	27.8

IET Sci. Meas. Technol., 2015, Vol. 9, Iss. 5, pp. 606–614

various currents are given in Table 7. Calculated data are in agreement with measured temperatures with a maximum error of 2.8% whereas CYMCAP shows a maximum error of 8.2%. As before, it is believed that the differences between the calculated and CYMCAP temperature are because of the use of different surface emissivity for the riser. In our calculations we used 0.6, which is the value provided in [19], whereas according to the technical support, CYMCAP uses a hard-coded emissivity of 0.9.

10 Conclusions

This paper has presented a circuit model for the thermal analysis of cables inside vertical, closed top and bottom, circular risers. The proposed circuit model is based on the thermal-electrical analogy and accounts for cable and riser thermal resistances to heat transfer by conduction and also for air non-linear thermal resistance in locations where both convection and radiation occur simultaneously. Indoor experiments on different cable and riser constructions with varied geometries were carried out for diverse load currents. Calculated and measured conductor temperatures are within 5%, establishing the validity of the proposed model and method.

It has been found by measurements and validated 3D FEM simulations that the riser height has an insignificant effect on the temperature of the conductor. Whereas, increasing the diameter of the riser yields reduced conductor temperatures. In addition, increasing the riser diameter leads to an increase of the per cent heat transferred by radiation and a reduction of the per cent heat transferred by convection. It is found, experimentally, that eccentric configuration has no significant effect on conductor temperature.

11 Acknowledgment

The authors would like to thank Mr. Rachit Vijay for his assistance performing the experiments.

12 References

1 IEEE Std. 835: 'Power cable ampacity tables', 1994, pp. 1678–1686
2 Hartline, R.A., Black, W.Z.: 'Ampacity of electric power cables in vertical protective risers', *IEEE Trans. Power Appl. Syst.*, 1983, PAS-102, (6), pp. 1678–1686
3 Kreith, F., Black, W.Z.: 'Basic heat transfer' (Harber & Row publishers, New York, 1980)
4 Anders, G.: 'Rating of cables on riser poles, in trays, in tunnels and shafts – A review', *IEEE Trans. Power Deliv.*, 1996, **11**, (1), pp. 3–11
5 CYMCAP Users' Guide version 5.04, CYME International T&D Inc. (St-Bruno, Quebec, 2010)
6 Cress, S.L., Motlis, J.: 'Temperature rise of submarine cable on riser poles', *IEEE Trans. Power Deliv.*, 1991, **6**, (1), pp. 25–33
7 De León, F.: 'Major factors affecting cable ampacity'. Power Engineering Society General Meeting, IEEE, 2006
8 Comsol Multiphysics: 'Heat transfer module user's guide' (Comsol AB Group, 2006), pp. 1–222
9 IEC Standard 60287-2-1: 'Electrical cables –Calculations of the current-rating-Part 2: Thermal resistance – Section 1: Calculation of the thermal resistance', 2001–11
10 Kays, W., Crawford, M.: 'Convective heat and mass transfer' (McGraw-Hill Series in Mechanical Engineering, New York, 1980, 2nd edn.)
11 Popiel, C.O.: 'Free convection from vertical slender cylinders: a review, heat transfer engineering', 2008, **29**, (6), pp. 521–536
12 Cebeci, T.: 'Laminar free convective heat transfer from the outer surface of a vertical slender circular cylinder'. Proc. Fifth Inst. Heat Transfer Conf., Tokyo, 1974, vol. 3, Paper NCI 1.4, pp. 15–19
13 Sparrow, E.M., Gregg, J.L.: 'Laminar free convection heat transfer from the outer surface of a vertical circular cylinder', *Trans. ASME*, 1956, **78**, pp. 1823–1829
14 Churchill, S.W., Chu, H.H.S.: 'Correlating equations for laminar and turbulent free convection from vertical flat plate', *Int. J. Heat Mass Transf.*, 1975, **18**, pp. 1323–1329
15 Power Engineering: 'Electrical power cable engineering', Thue, W. (ed.): (Washington, D.C., 1999)
16 Martynenko, O.G., Khramtsov, P.P.: 'Free convective heat transfer' (Springer-Verlag, Berlin, Germany, 2005)
17 Holman, J.P.: 'Heat transfer' (McGraw-Hill, New York, 1986, 6th edn.)
18 Vahl Davis, G. de, Thomas, R.W.: 'Natural convection between concentric vertical cylinders', *Phys. Fluids 12, II-198*, 1969; doi: 10.1063/1.1692437
19 IEC Standard 60287-1-1: 'Electric cables-calculation of the current rating-part 1: current rating equations (100% load factor) and calculation of losses-section 1: general', 1994–12
20 Anders, G.: 'Rating of electric power cables in unfavorable thermal environment' (Wiley-IEEE press, 2005)

13 Appendix

13.1 Appendix 1: Cables and risers data

See Fig. 9 and Table 8.

13.2 Appendix 2

Garshoff number

$$G_H = \left[\frac{g(\Delta\theta)\beta L^3}{\nu^2}\right] \tag{21}$$

Reynolds number

$$Ra_H = (\mathrm{Pr})(G_H) \tag{22}$$

where g is the acceleration of gravity m/s^2, β is the volumetric thermal expansion coefficient 1/°C, ν is the kinematic viscosity m^2/s, L is length of the cable IR m, and P_r dimensionless Prandtl number. Air thermal properties β, ν and Pr are provided in [10] and must be selected for proper film temperature.

The physical properties of the cable and riser materials are provided by IEC Standard 60287-1-1 [19] and copied below for completeness.

Properties of Cable type-A

Table 8 Data of risers

	Type-I	Type-II
inner diameter	51.19 mm	101.6 mm
outer diameter	60.28 mm	114.4 mm
material	PVC	PVC

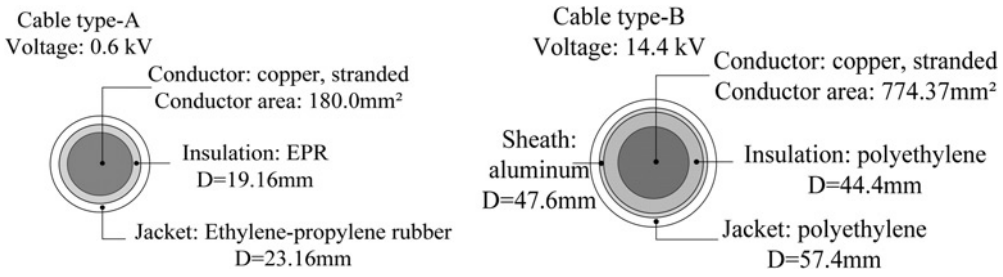

Fig. 9 *Cable type-A and cable type-B*

r_c–Radius of copper conductor, 7.6 mm.
r_d–Outer radius of the EPR insulation, 9.6 mm.
r_s–Outer radius of the jacket, 11.60 mm.
L–Length of cable IR, 2.0 m.
k_d–EPR thermal conductivity, 0.20 W/(m°C).
k_s–Jacket thermal conductivity, 0.20 W/(m°C).
ρ_c–Resistivity of copper at 20°C, 1.7241×10^{-8} Ω.m
α_{20}–Temperature coefficient per K at 20°C, 3.93×10^{-3}
$\in$–Relative permittivity of the insulation, 3.0
ε_s–Emissivity of the cable surface, 0.90
σ–Stefan–Boltzmann's constant, 5.667×10^{-8}

Properties of riser type-I

r_{IR}–Riser inner radius, 25.59 mm
r_{OR}–Riser outer radius, 30.14 mm
k_R–Riser thermal conductivity, 0.1667 W/(m°C)
ε_s–Emissivity of the PVC, 0.60

Electrical properties

f–Frequency = 60 Hz
I_c–Load current = 500 A
U_0–Voltage to ground (V), 14.4 kV

IET Sci. Meas. Technol., 2015, Vol. 9, Iss. 5, pp. 606–614